

TRACKING QUINTESSENCE

ARTUR ALHO,^{1*} CLAES UGGLA,^{2†} AND JOHN WAINWRIGHT^{3‡}

¹*Center for Mathematical Analysis, Geometry and Dynamical Systems,*

Instituto Superior Técnico, Universidade de Lisboa,

Av. Rovisco Pais, 1049-001 Lisboa, Portugal.

²*Department of Physics, Karlstad University,*

S-65188 Karlstad, Sweden.

³*Department of Applied Mathematics, University of Waterloo,*

Waterloo, ON, N2L 3G1, Canada.

Abstract

Tracking quintessence, in a spatially flat and isotropic space-time with a minimally coupled canonical scalar field and an asymptotically inverse power-law potential $V(\varphi) \propto \varphi^{-p}$, $p > 0$, as $\varphi \rightarrow 0$, is investigated. This is done by introducing a new three-dimensional *regular* dynamical system, which enables a rigorous explanation of the tracking feature: 1) The dynamical system has a tracker fixed point T with a two-dimensional stable manifold that pushes an open set of nearby solutions toward a single tracker solution originating from T. 2) All solutions, including the tracker solution and the solutions that track/shadow it, end at a common future attractor fixed point that depends on the potential. Thus, the open set of solutions that shadow the tracker solution share its properties during the tracking quintessence epoch. We also discuss similarities and differences of underlying mechanisms for tracking, thawing and scaling freezing quintessence, and, moreover, we illustrate with state space pictures that all of these types of quintessence exist simultaneously for certain potentials.

1 Introduction

In 1998 observations of type Ia supernovae indicated that the Universe is presently accelerating [1, 2]. Within the framework of General Relativity this cosmic acceleration implies that there exists an exotic energy component in the Universe, called dark energy, with an equation of state parameter satisfying $w_{\text{DE}} < -1/3$. The simplest candidate for dark energy, apart from a cosmological constant, is a dynamical canonical scalar field φ , minimally coupled to gravity and with a potential $V(\varphi)$, referred to as quintessence, Caldwell *et al.* (1998) [3] (for reviews and references about quintessence, see *e.g.*

*Electronic address: aalho@math.ist.utl.pt

†Electronic address: claes.uggla@kau.se

‡Electronic address: jwainwri@uwaterloo.ca

Tsujikawa (2013) [4] and Bahamonde *et al.* (2018) [5]). At the present time the energy density of quintessence and matter are roughly of the same size ($\Omega_\varphi \approx 0.7$, $\Omega_m \approx 0.3$) which raises the need to explain this near coincidence without specifying precise initial conditions. To address this difficulty Zlatev *et al.* (1999) [6], and Steinhardt *et al.* (1999) [7] showed that for potentials with the property $V(\varphi) \propto \varphi^{-p}$, $p > 0$, as $\varphi \rightarrow 0$, the quintessence governing equations have a special solution they called a tracker solution since it attracts solutions that then track/shadow it for a wide range of initial conditions. A second property the tracker solution exhibit is that the scalar field equation of state parameter w_φ is nearly constant in the matter-dominated epoch and less than w_m , the equation of state parameter of the background matter. This implies that the energy density ρ_m decreases faster than ρ_φ so that as the universe evolves from matter-domination ρ_φ will catch up and overtake ρ_m . Taken together these two properties go some way toward solving the coincidence problem. This type of evolution is referred to as *tracking quintessence*.¹

In this paper we give a description of tracking quintessence by means of a new *regular* dynamical systems framework that is valid for asymptotically inverse power-law potentials, $V(\varphi) \propto \varphi^{-p}$, $p > 0$, as $\varphi \rightarrow 0$.² We use our new regular dynamical systems framework to show that there exists a unique tracker solution with the properties of the heuristically defined tracker solution of Steinhardt and co-workers, originating from a new *hyperbolic tracker fixed point*. The fact that all the eigenvalues of this isolated fixed point have non-zero real parts makes it possible to i) explain the tracking feature and ii) obtain analytic approximate expressions for tracker solutions. Moreover, the global and regular structure of the state space shows explicitly a) the entire tracker solution and gives insight into the possible initial conditions which lead to solutions that approach the tracker fixed point and then track/shadow the tracker solution; b) that these models also give rise to thawing quintessence solutions, and that some potentials belonging to the present class simultaneously in addition give rise to co-existing scaling freezing quintessence solutions.

The outline of the paper is as follows. In the next section we derive the new regular dynamical system. In Section 3 we briefly review the tracker conditions of Steinhardt and co-workers [7, 6] and describe the general structure of the new state space, including the fixed points of the dynamical system that determine the intermediate and late time behaviour of the quintessence solutions. In Section 4 we give a general dynamical systems description of thawing, scaling freezing and tracking quintessence, focussing on the latter, and in Section 5 we give specific examples that illustrate the previous general

¹We note that prior to the development of the concept of tracker quintessence Peebles and Ratra (1988) [8] and [9] studied scalar field cosmologies with matter and showed that for the inverse power-law potential when $\rho_\varphi \ll \rho_m$ one obtains $\rho_\varphi/\rho_m \sim e^{6/(2+p)N}$, which shows that ρ_φ decreases more slowly than ρ_m as the universe expands and will eventually become dominant. This is consistent with the ‘tracker’ expression $w_\varphi := p_\varphi/\rho_\varphi = -2/(2+p)$, first derived by Ratra and Quillen (1992) [10], eq. (5), and then by Steinhardt *et al.* (1999) [7] for the inverse power-law potential, see also Podario and Ratra (2000) [11] and Peebles and Ratra (2003) [12].

²This paper complements our recent paper Alho, Uggla and Wainwright (2023) [13] which deals with potentials for which $\lambda(\varphi) = -V_{,\varphi}/V$ is bounded and $\varphi \in (-\infty, \infty)$, referred to as AUW [13]. This is in contrast both physically and mathematically to the present asymptotically inverse power-law potentials, which yield an extremely steep potential wall when $\varphi \rightarrow 0$, resulting in $\varphi \in (0, \infty)$ instead of $\varphi \in (-\infty, \infty)$.

discussion using three-dimensional state space figures and graphs of w_φ . Finally, there is a brief concluding Section 6.

2 A regular dynamical system for unbounded λ

Consider a spatially flat and isotropic Robertson-Walker spacetime with a source that consists of matter with an energy density $\rho_m > 0$ and pressure $p_m = 0$, which represents cold dark matter,³ and a minimally coupled canonical scalar field, φ , with a potential $V(\varphi) > 0$, which results in the following energy density and pressure

$$\rho_\varphi = \frac{1}{2}\dot{\varphi}^2 + V(\varphi), \quad p_\varphi = \frac{1}{2}\dot{\varphi}^2 - V(\varphi), \quad (1)$$

where an overdot represents the derivative with proper time t . For these models, the Raychaudhuri equation, the Friedmann equation, the non-linear Klein-Gordon equation, and the energy conservation law for matter with zero pressure, can be written as⁴

$$\dot{H} + H^2 = -\frac{1}{6}(\rho + 3p), \quad (2a)$$

$$3H^2 = \rho, \quad (2b)$$

$$\ddot{\varphi} = -3H\dot{\varphi} - V_{,\varphi}, \quad (2c)$$

$$\dot{\rho}_m = -3H\rho_m, \quad (2d)$$

where the Hubble variable is defined by $H = \dot{a}/a$, and the total energy density ρ and pressure p are given by

$$\rho = \rho_\varphi + \rho_m, \quad p = p_\varphi. \quad (3)$$

Our dynamical system is based on three key quantities associated with the scalar field: the scalar field equation of state parameter $w_\varphi := p_\varphi/\rho_\varphi$, the Hubble-normalized energy density Ω_φ and scalar field potential Ω_V :

$$1 + w_\varphi := \frac{\rho_\varphi + p_\varphi}{\rho_\varphi} = \frac{\varphi'^2}{3\Omega_\varphi}, \quad \text{provided that } \Omega_\varphi > 0, \quad (4a)$$

$$\Omega_\varphi := \frac{\rho_\varphi}{3H^2} = \frac{1}{6}\varphi'^2 + \Omega_V, \quad (4b)$$

$$\Omega_V := \frac{V}{3H^2} = \frac{1}{2}(1 - w_\varphi)\Omega_\varphi, \quad (4c)$$

where a $'$ denotes the derivative with respect to e -fold time, $N := \ln(a/a_0)$, where a is the cosmological scale factor and $a_0 = a(t_0)$ is its value at the present time, given by $N = 0$. It follows from (1) and (4) and the assumed positivity of V that

$$1 + w_\varphi \geq 0, \quad 1 - w_\varphi > 0. \quad (5)$$

³This simple model is useful for describing the transition from an epoch of matter-domination to an epoch in which the scalar field is dominant. A more realistic model requires a two component source with matter and radiation leading to a four-dimensional state space, as described in [14].

⁴We use units such that $c = 1$ and $8\pi G = 1$, where c is the speed of light and G is the gravitational constant.

When using equations (2) we will convert from proper time t to e -fold time N using

$$\partial_t = H\partial_N, \quad \partial_t^2 = H^2[\partial_N^2 - (1+q)\partial_N], \quad (6)$$

where the *deceleration parameter* q is defined by

$$1+q := -\frac{\dot{H}}{H^2}. \quad (7)$$

In particular (2c) assumes the form

$$\varphi'' + (2-q)\varphi' - 3\lambda(\varphi)\Omega_V = 0, \quad (8)$$

where $\lambda(\varphi)$ is defined by

$$\lambda := -\frac{V_{,\varphi}}{V}. \quad (9)$$

We also need the Hubble-normalized matter density Ω_m and its evolution equation, given by

$$\Omega_m := \frac{\rho_m}{3H^2} = 1 - \Omega_\varphi, \quad \Omega'_m = (2q-1)\Omega_m, \quad (10)$$

as follows from (2d) and (7). The deceleration parameter q can be expressed as

$$1+q = \frac{3}{2}(1+w_\varphi\Omega_\varphi), \quad (11)$$

as follows from (7) in conjunction with (1), (2) and (3).

Equation (4a), which can be written as

$$(\varphi')^2 = 3\Omega_\varphi(1+w_\varphi), \quad (12)$$

relates φ' to Ω_φ and w_φ , which satisfy the differential equations⁵

$$\Omega'_\varphi = -3w_\varphi(1-\Omega_\varphi)\Omega_\varphi, \quad (13a)$$

$$w'_\varphi = -3(1-w_\varphi)\left(1+w_\varphi - \frac{1}{3}\lambda(\varphi)\varphi'\right). \quad (13b)$$

As in AUW [13], since $1+w_\varphi \geq 0$ we can replace w_φ by a variable u according to

$$u^2 := 1+w_\varphi, \quad (14)$$

with the stipulation that u has the *same sign* as φ' . It follows from (12) that

$$\varphi' = \sqrt{3\Omega_\varphi}u, \quad (15)$$

which leads to that (13b) takes the form

$$u' = \frac{3}{2}(2-u^2)\left(\lambda(\varphi)\sqrt{\Omega_\varphi/3} - u\right). \quad (16)$$

⁵Equation (13a) follows from (10) and (7); equation (13b) is obtained by differentiating (12) and using (13a) and (8).

In this paper we consider positive asymptotically inverse power-law potentials for which λ has the following divergence as $\varphi \rightarrow 0$:

$$\lim_{\varphi \rightarrow 0} \varphi \lambda = p, \quad (17a)$$

with $p > 0$ where $\lambda(\varphi)$ is subsequently assumed to be bounded with a finite limit as $\varphi \rightarrow \infty$,

$$\lim_{\varphi \rightarrow \infty} \lambda = \lambda_+. \quad (17b)$$

Next we replace the unbounded scalar field variable $\varphi \in [0, \infty)$ by a bounded variable $\bar{\varphi} \in [0, 1]$. We do this by choosing a regular, increasing (and hence invertible) function $\bar{\varphi}(\varphi)$ with $\varphi \in [0, \infty)$. The choice of $\bar{\varphi}(\varphi)$ is guided by the form of $\lambda(\varphi)$, but is required to satisfy the following conditions:

$$\bar{\varphi}(0) = 0, \quad \left. \frac{d\bar{\varphi}}{d\varphi} \right|_{\varphi=0} = b > 0, \quad \lim_{\varphi \rightarrow \infty} \bar{\varphi}(\varphi) = 1, \quad \lim_{\varphi \rightarrow \infty} \left(\frac{d\bar{\varphi}}{d\varphi} \right) = 0. \quad (18)$$

We will regard the derivative $d\bar{\varphi}/d\varphi$ as a function of $\bar{\varphi}$ which we denote by $F(\bar{\varphi})$:

$$F(\bar{\varphi}) := \frac{d\bar{\varphi}}{d\varphi}, \quad \text{with } F(0) = b, \quad F(1) = 0, \quad (19)$$

where the two equalities follow from (18). Hence (15) assumes the form

$$\bar{\varphi}' = \sqrt{3\Omega_\varphi} u F(\bar{\varphi}). \quad (20)$$

We now come to the main new ingredient in our new dynamical systems formulation where we use the growth condition (17a) to regularize equations (16) and (20). It follows from (17a) that⁶ $\lim_{\bar{\varphi} \rightarrow 0} (\bar{\varphi} \lambda(\bar{\varphi})) = pb$, where, with a slight abuse of notation, $\lambda(\bar{\varphi}) = \lambda(\varphi(\bar{\varphi}))$. This makes it possible to define a regular function $G(\bar{\varphi})$ according to

$$G(\bar{\varphi}) := \bar{\varphi} \lambda(\bar{\varphi}), \quad \text{for } 0 < \bar{\varphi} \leq 1, \quad G(0) = pb, \quad (21a)$$

while (17b) and (18) leads to $\lambda|_{\bar{\varphi}=1} = \lambda_+$ and hence that

$$G(1) = \lambda_+. \quad (21b)$$

We then use (21a) to replace λ by G in (16), which suggests that we define a new *positive* variable v by writing

$$\Omega_\varphi = 3v^2 \bar{\varphi}^2, \quad v := \frac{1}{\bar{\varphi}} \sqrt{\frac{\Omega_\varphi}{3}}. \quad (22)$$

After substituting the above expression for Ω_φ in (16) and (20) we obtain regular equations for u' and $\bar{\varphi}'$. The final step is to differentiate (22) and use (13a) and (20)

⁶Use $\lim_{\bar{\varphi} \rightarrow 0} (\bar{\varphi}/\varphi) = b$, which follows from the second equation in (18).

to calculate v' . On collecting the results, the regular system of equations for the state vector $(\bar{\varphi}, u, v)$ has the following form:

$$\bar{\varphi}' = 3uv\bar{\varphi}F(\bar{\varphi}), \quad (23a)$$

$$u' = \frac{3}{2}(2 - u^2)(vG(\bar{\varphi}) - u), \quad (23b)$$

$$v' = \frac{3}{2}[(1 - u^2)(1 - 3v^2\bar{\varphi}^2) - 2uvF(\bar{\varphi})]v, \quad (23c)$$

where $F(\bar{\varphi})$ and $G(\bar{\varphi})$ are defined by (19) and (21a).

We conclude this section by noticing that tracking quintessence was discovered in connection with the inverse power-law potential $V \propto \varphi^{-p}$, $p > 0$. To treat these models in the present dynamical systems setting we can follow [15] and define $\bar{\varphi}$ as

$$\bar{\varphi} := \frac{\varphi}{1 + \varphi}, \quad (24)$$

which results in a regular dynamical system with

$$F = (1 - \bar{\varphi})^2, \quad G = p(1 - \bar{\varphi}), \quad (25)$$

from which it follows that $F(0) = 1$, and thereby $b = 1$, $G(0) = p$, $G(1) = 0$.

3 Tracker conditions and general dynamical systems features

3.1 Tracker conditions

Steinhardt and co-workers [7, 6] introduced the concept of *tracking quintessence*, which entailed that a wide range of initial conditions result in solutions that are attracted to a special solution called the tracker solution. The analysis in Steinhardt *et al.* [7] uses the scalars Δ and Γ , defined by:

$$\Delta := \pm\lambda \sqrt{\frac{\Omega_\varphi}{3(1 + w_\varphi)}}, \quad \Gamma := \frac{V_{,\varphi\varphi}}{V_{,\varphi}^2} = 1 + (\lambda^{-1})_{,\varphi} \quad (26)$$

(for Δ , see equation (9) in [7]). The definition of Δ results in that the evolution equation for w_φ can be written in the form

$$w'_\varphi = -3(1 - w_\varphi^2)(1 - \Delta), \quad (27)$$

while if $w'_\varphi = 0$ and $1 + w_\varphi > 0$ then⁷

$$\Gamma - 1 = \frac{(w_m - w_\varphi)(1 - \Omega_\varphi)}{2(1 + w_\varphi)}. \quad (28)$$

⁷See equation (33) in Rubano *et al.* (2004) [16].

In the approach of Steinhart *et al.* [7] tracking quintessence is described by the conditions

$$\Delta \approx 1 \quad \text{and} \quad \Gamma - 1 > 0. \quad (29)$$

Heuristically, the first condition implies that w_φ is nearly constant, and hence that (28) holds approximately, which, due to the second tracker condition, $\Gamma - 1 > 0$, suggests that $w_\varphi < w_m$, where $w_m = 0$ in the present paper results in $w_\varphi < 0$. This condition is in turn important since it implies that, as long as the conditions hold, $\Omega'_\varphi > 0$ according to (13a) so that Ω_φ increases as the universe ages. Finally, the second condition, $\Gamma - 1 = (\lambda^{-1})_{,\varphi} > 0$, corresponds to that λ is monotonically decreasing. In terms of our state space variables the scalar Δ becomes

$$\Delta = \bar{\varphi} \lambda(\bar{\varphi}) \left(\frac{v}{u} \right) = G(\bar{\varphi}) \left(\frac{v}{u} \right). \quad (30)$$

3.2 State space features

Recall that the dynamical system (23) asymptotically depends on the three parameters $b = F(0)$, $\lambda_+ = G(1)$ and p via $G(0) = pb$, where b is associated with the bounded scalar field variable $\bar{\varphi}$, while λ_+ and p characterize the asymptotic properties of the scalar field potential $V(\bar{\varphi})$. The state space of the system (23) is described by the bounded variables $\bar{\varphi} \in [0, 1]$, $u \in [-\sqrt{2}, \sqrt{2}]$, and the unbounded variable $v \in [0, \infty)$. There are six invariant boundary sets:

$$\bar{\varphi} = 0, \quad \bar{\varphi} = 1, \quad u = \pm\sqrt{2}, \quad v = 0, \quad v = \frac{1}{\sqrt{3}\bar{\varphi}}. \quad (31)$$

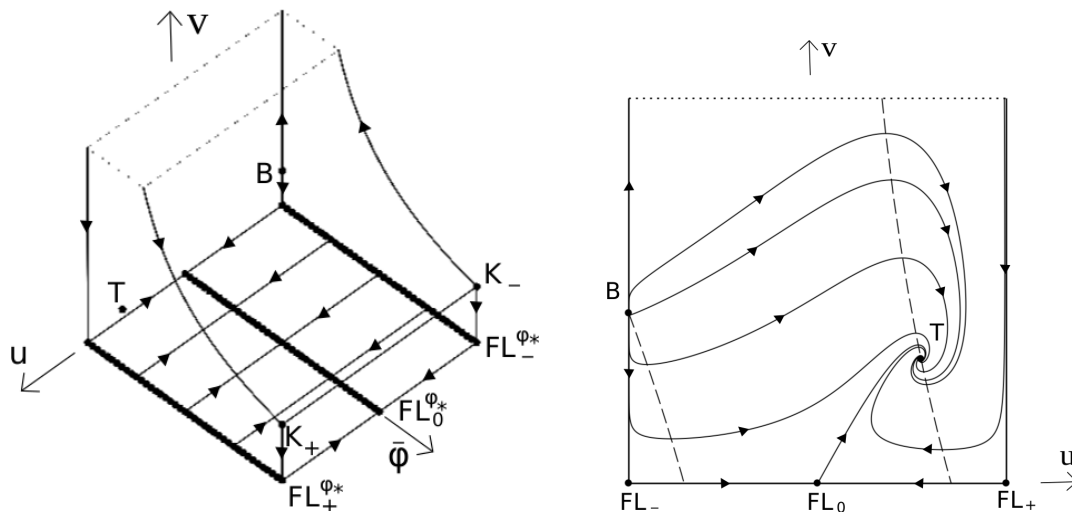
Thinking of $(\bar{\varphi}, u, v)$ as Cartesian coordinates the state space can be visualized as a three-dimensional solid, with rectangular base $v = 0$, vertical sides $u = \pm\sqrt{2}$, and vertical ends $\bar{\varphi} = 0, 1$. The solid is bounded above by the curved ‘ski-slope surface’ $v = 1/\sqrt{3}\bar{\varphi}$, $0 < \bar{\varphi} \leq 1$, with $v \rightarrow \infty$ as $\bar{\varphi} \rightarrow 0$. We will refer to this three-dimensional solid as the ‘ski-slope state space’.

The relation (22), $\Omega_\varphi = 3v^2\bar{\varphi}^2$, provides a physical interpretation of some of the boundary sets. First, on the sets $v = 0$ and $\bar{\varphi} = 0$ we have $\Omega_\varphi = 0$, and hence $\Omega_m = 1$. Thus the subset on which the *matter is dominant* ($\Omega_m = 1$) is the union of the boundary sets $v = 0$ and $\bar{\varphi} = 0$. Second, the ski-slope surface $v = 1/\sqrt{3}\bar{\varphi}$ is the boundary set on which the *scalar field is dominant*, since $\Omega_\varphi = 1$. To continue, it follows from (14) that the sets $u = \pm\sqrt{2}$ are characterized by $w_\varphi = 1$ and hence, as follows from (4c), $\Omega_V = 0$. Finally, recall that λ has a constant value λ_+ on the invariant set $\bar{\varphi} = 1$, which is therefore referred to as *the exponential potential boundary set*.

We note that there is a mathematical common ground between the present paper and AUW [13]. In particular, the boundary sets $v = 0$, on which $\bar{\varphi} = \text{constant}$, and $\bar{\varphi} = 1$ are *identical* to the same boundary sets in AUW [13].⁸ The solution space

⁸This can be seen by comparing the current system (23) with the corresponding system given by equations (20) in AUW [13], but note that the domain of $\bar{\varphi}$ (and φ) is different. Although u is the same in AUW as here, this is not the case with v . Since v in AUW [13] is given by $v(\text{AUW}) = \sqrt{\Omega_\varphi/3}$ it follows that the present v and $v(\text{AUW})$ are related by $v = v(\text{AUW})/\bar{\varphi}$. Thus $v = v(\text{AUW})$ when $\bar{\varphi} = 1$, but note that it is the factor $\bar{\varphi}^{-1}$ in $v = v(\text{AUW})/\bar{\varphi} \rightarrow v(\text{AUW})/\varphi$ when $\varphi \rightarrow 0$ that regularizes the present dynamical system at $\varphi = 0$, which enables our results concerning the tracker solution.

structures on the exponential boundary arising from different values of λ_+ were dealt with in detail in AUW and in [17], and we will therefore not discuss them in this paper. Figure 1 illustrates some key features of the ski-slope state space; note that the solution space structure on the boundaries $v = 0$ and $u = \pm\sqrt{2}$ is independent of λ and thereby on the potential.



(a) The ski-slope state space with the six boundary sets in (31). Depicted are also solution trajectories on the $v = 0$ subset with $\bar{\varphi} = \text{constant}$, which are independent of the potential, as are the solution trajectories on the $u = \pm\sqrt{2}$ boundaries.

(b) The solution space structure on the $\bar{\varphi} = 0$ boundary, where there are no bifurcations as $b > 0$ and $p > 0$ change. The dashed curves show where $v' = 0$; v is increasing (decreasing) between (outside) the two $v' = 0$ curves. On this boundary the fixed point B is a source while T is a sink.

Figure 1: The ski-slope state space and the $\bar{\varphi} = 0$ boundary. The dotted lines correspond to a cut off in v in order to obtain a finite figure, since $v \rightarrow \infty$ when $\bar{\varphi} \rightarrow 0$, which also results in a cut off for small $\bar{\varphi}$ on the scalar field dominant boundary $v\bar{\varphi} = 1/\sqrt{3}$.

Since the scalar field potential is not exponential, the scalar field contributes a source that is not scale-invariant. From this it follows that the Hubble scalar H is a function of the state vector $(\bar{\varphi}, u, v)$. By using (4c) in conjunction with (14) and (22) we obtain

$$3H^2 = \frac{V}{\Omega_V} = \frac{2V}{(1 - w_\varphi)\Omega_\varphi} = \frac{2V(\bar{\varphi})}{3(2 - u^2)v^2\bar{\varphi}^2}, \quad (32)$$

where

$$(3H^2)' = -2(1 + q)(3H^2) = -3(1 + w_\varphi\Omega_\varphi)(3H^2) = -3[1 + 3(u^2 - 1)v^2\bar{\varphi}^2](3H^2), \quad (33)$$

as follows from the definitions of the new variables and (11). In the interior state space, where $\Omega_\varphi < 1$ and $-1 \leq w_\varphi < 1$, it follows that $1 + q > 0$ and hence that $3H^2(u, v, \bar{\varphi})$ is monotonically decreasing. Thus, there are no periodic orbits (*i.e.* solution trajectories) or fixed points in the interior state space and hence all fixed points of the dynamical system (23) lie on the boundary of the ski-slope state space, given by (31) (in addition, an asymptotic analysis shows that there are no interior orbits that end at $\bar{\varphi} = 0$ and $v = +\infty$).

3.3 Fixed points of the dynamical system

Some of the fixed points of the dynamical system (23) depend on λ and thereby on the positive potential. Although not necessary, apart from the asymptotic condition (17a) we, for simplicity, assume that the potentials also satisfy the second condition (17b) and that the potentials are

- (i) *monotonically decreasing, i.e.* $V_{,\varphi} < 0$ and hence $\lambda(\varphi) > 0$, or
- (ii) *have a single positive minimum, i.e.* there exists a positive finite $\varphi = \varphi_0$ such that $V_{,\varphi}|_{\varphi=\varphi_0} = 0$ and $V_{,\varphi\varphi}|_{\varphi=\varphi_0} > 0$ and hence $\lambda(\varphi_0) = 0$, $\lambda_{,\varphi}|_{\varphi=\varphi_0} < 0$.⁹

The matter dominant boundary $v = 0$

It follows from (23) that the boundary set $v = 0$ is independent of λ and thereby also on the potential and that $v = 0$ contains three Friedmann-Lemaître lines of fixed points:

$$\text{FL}_0^{\varphi_*}: \quad (\bar{\varphi}, u, v) = (\bar{\varphi}_*, 0, 0), \quad (34a)$$

$$\text{FL}_{\pm}^{\varphi_*}: \quad (\bar{\varphi}, u, v) = (\bar{\varphi}_*, \pm\sqrt{2}, 0), \quad (34b)$$

where the constant $\bar{\varphi}_*$ satisfies $0 \leq \bar{\varphi}_* \leq 1$. Note that $w_{\varphi} = -1$ on $\text{FL}_0^{\varphi_*}$ while $w_{\varphi} = 1$ on $\text{FL}_{\pm}^{\varphi_*}$. These fixed points correspond to the fixed points with the same labels in AUW [13] (see equations (24)). The lines of fixed points are connected by heteroclinic orbits (a heteroclinic orbit is a solution trajectory that connects two different fixed points) $\text{FL}_{\pm}^{\varphi_*} \rightarrow \text{FL}_0^{\varphi_*}$ that are straight lines with ‘frozen’ scalar field values $\bar{\varphi} = \bar{\varphi}_* = \text{constant}$. The orbit structure on the boundary $v = 0$ is shown in Figure 1(a).

The matter dominant boundary $\bar{\varphi} = 0$

The boundary set $\bar{\varphi} = 0$ reflects the unboundedness of λ , and this gives rise to new fixed points with $v > 0$, as follows from (23):

$$\text{T}: \quad (\bar{\varphi}, u, v) = u_{\text{T}} \left(0, 1, \frac{1}{pb} \right), \quad u_{\text{T}} = \sqrt{\frac{p}{2+p}}, \quad (35a)$$

$$\text{B}: \quad (\bar{\varphi}, u, v) = \sqrt{2} \left(0, -1, \frac{1}{4b} \right), \quad (35b)$$

where $b = F(0) > 0$ is the constant defined in (19). *On the boundary set $\bar{\varphi} = 0$, a local analysis shows that the fixed point T is a spiral sink,¹⁰ B is a source (although B is a saddle in the full state space) and the three FL fixed points with $v = 0$ are saddles. We conjecture that all interior orbits in the boundary set $\bar{\varphi} = 0$ are attracted to T. Although the details of the orbit structure on $\bar{\varphi} = 0$ depend on the parameters p and b , there are no bifurcations as the parameters change and thus the qualitative orbit structure on $\bar{\varphi} = 0$ is independent of the potential; a representative description is shown in Figure 1(b) using the values $b = 1$ and $p = 3$.*

⁹Incidentally, as far as we know, asymptotically inverse power-law potentials with a positive minimum have not been investigated before in the literature.

¹⁰The eigenvalues associated with T on the boundary $\bar{\varphi} = 0$ are rather complicated but can conveniently be described as follows: $\lambda_1 + \lambda_2 = -\frac{3}{2} \left(\frac{p+4}{p+2} \right) - 3u_{\text{T}}b$, $\lambda_1\lambda_2 = \frac{9}{2}(p+4)u_{\text{T}}b$.

The exponential boundary $\bar{\varphi} = 1$

We have already noted that this boundary set coincides with the boundary set $\bar{\varphi} = 1$ in AUW [13]. We briefly summarize the fixed points: apart from the $\bar{\varphi} = 1$ boundary end points of the matter-dominated FL lines of fixed points with $v = 0$ there are additional fixed points on the exponential $\bar{\varphi} = 1$ boundary: the scalar field dominated ‘kinaton’ fixed points K_{\pm} , the de Sitter fixed point dS (when $\lambda_+ = 0$), the power-law fixed point P (when $0 < |\lambda_+| < \sqrt{6}$), and the scaling fixed point S (when $|\lambda_+| > \sqrt{3}$). The values of u and v for the fixed points on the $\bar{\varphi} = 1$ boundary are:

$$K_{\pm}: \quad (u, v) = \left(\pm\sqrt{2}, \frac{1}{\sqrt{3}} \right), \quad (36a)$$

$$\text{dS}: \quad (u, v) = \left(0, \frac{1}{\sqrt{3}} \right), \quad \lambda_+ = 0, \quad (36b)$$

$$\text{P}: \quad (u, v) = \frac{1}{\sqrt{3}}(\lambda_+, 1), \quad 0 < |\lambda_+| < \sqrt{6}, \quad (36c)$$

$$\text{S}: \quad (u, v) = \left(\text{sgn}(\lambda_+), \frac{1}{|\lambda_+|} \right), \quad |\lambda_+| > \sqrt{3}. \quad (36d)$$

Details and figures depicting the orbit structures for the different cases associated with $\lambda_+ = 0$, $0 < |\lambda_+| < \sqrt{3}$, $\sqrt{3} < |\lambda_+| < \sqrt{6}$, $\sqrt{6} < |\lambda_+|$ on the exponential boundary $\bar{\varphi} = 1$ are given in AUW [13] while global results were proven in [17]. For monotonically decreasing potentials P is a sink (as is dS with $q = -1$ when $\lambda_+ = 0$); since $q = -1 + \lambda_+^2/2$ at P it follows that $\lambda_+ < \sqrt{2}$ results in future eternal acceleration, which we, for simplicity, henceforth assume when the potential is monotonically decreasing.

The scalar field dominant boundary $v\bar{\varphi} = 1/\sqrt{3}$

For monotonically decreasing scalar field potentials with $\lambda(\varphi) > 0$ and $0 \leq \lambda_+ < \sqrt{2}$, the function $3H^2$ in (33) is also a monotonic function on the interior of this boundary, although the evolution of $3H^2$ goes through an inflection point for orbits when and if they pass through $u = 0$, which they only can do once since $u'|_{u=0} > 0$, and hence there are no periodic orbits or fixed points in the interior of the scalar field dominant boundary in this case.

Let us now turn to the case of a scalar field potential with a positive minimum. Apart from the previous fixed points, the minimum results in an additional fixed point given by

$$\text{dS}^0: \quad (\bar{\varphi}, u, v) = \left(\bar{\varphi}_0, 0, \frac{1}{\sqrt{3}\bar{\varphi}_0} \right), \quad (37)$$

where $\lambda(\bar{\varphi}_0) = 0$, $\bar{\varphi}_0 \in (0, 1)$, at the minimum of the potential. Since $\lambda_{,\varphi}|_{\bar{\varphi}=\bar{\varphi}_0} = -(V_{,\varphi\varphi}/V)|_{\bar{\varphi}=\bar{\varphi}_0}$ it follows that $\lambda_{,\varphi}|_{\bar{\varphi}=\bar{\varphi}_0} < 0$ yields a positive minimum of the potential, and when this is the case, which we assume, the eigenvalues associated with dS^0 have negative real parts and therefore dS^0 is then a sink,¹¹ which is a spiral on the scalar field dominant boundary if $\lambda_{,\varphi}|_{\bar{\varphi}=\bar{\varphi}_0} < -3/4$. When $-\sqrt{6} < \lambda_+ < 0$ the fixed point P exists, with one orbit originating from it (P is replaced with dS if $\lambda_+ = 0$) on the scalar

¹¹The eigenvalues of the fixed point dS^0 are $-(3/2) \left(1 \pm \sqrt{1 + (4/3)\lambda_{,\varphi}|_{\bar{\varphi}=\bar{\varphi}_0}} \right)$, -3 , where the eigenvectors of the first pair are tangential to the scalar field dominant boundary while the eigenvector connected with the eigenvalue -3 corresponds to the Λ CDM orbit associated with the positive minimum of the scalar field potential V .

field dominant boundary, but this fixed point leaves the state space when $\lambda_+ = -\sqrt{6}$, which results in that all orbits on the scalar field dominant boundary (apart from the fixed point dS^0) originate from an asymptotic cycle of boundary orbits and the limit $v \rightarrow +\infty$ where u is monotonically increasing when $\lambda_+ \leq -\sqrt{6}$, see Figure 2.¹²

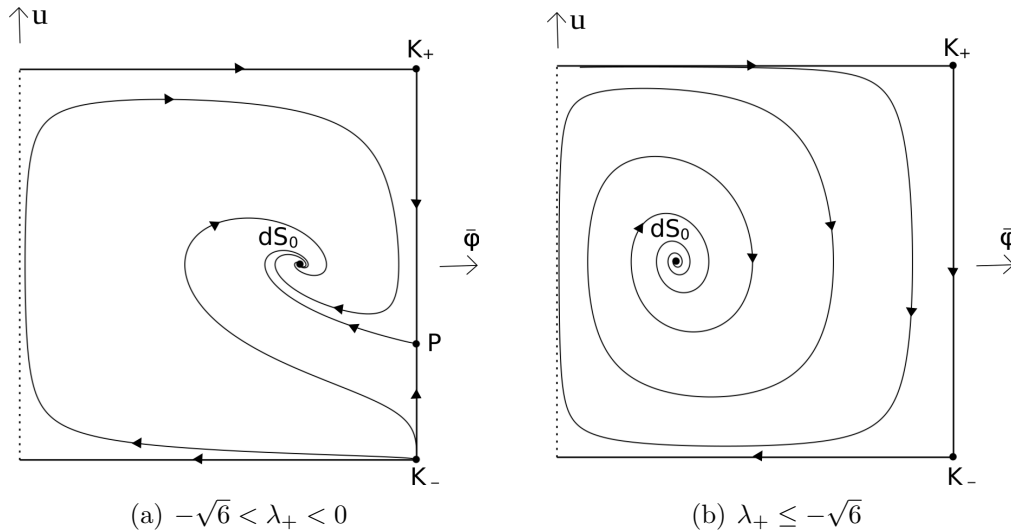


Figure 2: The orbit structure on the scalar field dominant boundary $v\bar{\varphi} = 1/\sqrt{3}$ projected onto $(\bar{\varphi}, u)$ with $0 < \bar{\varphi} \leq 1$ on the horizontal axis and $u \in [-\sqrt{2}, \sqrt{2}]$ on the vertical axis for the cases $-\sqrt{6} < \lambda_+ < 0$ and $\lambda_+ \leq -\sqrt{6}$, respectively. These two cases are illustrated by the models given in eq. (39) with $p = 1/2$, $\nu = 2$ and the two values $\alpha = -1$ and $\alpha = -10$, which result in $\lambda_+ = -1$ and $\lambda_+ = -10$, respectively, since $\lambda_+ = p\nu\alpha$ for these models. The dotted line corresponds to the cut off in $\bar{\varphi}$ on the scalar field dominant boundary in Figure 1.

We conclude this section by first summarizing the values of Ω_φ and w_φ at the fixed points:

$$\Omega_\varphi = 1: \quad P, dS, dS^0, K_\pm \quad \text{with} \quad w_\varphi = \frac{\lambda_\pm^2}{3} - 1, -1, -1, 1, \quad (38a)$$

$$\Omega_\varphi = 0: \quad FL_0^{\varphi*}, FL_\pm^{\varphi*}, T, B \quad \text{with} \quad w_\varphi = -1, 1, -\frac{2}{2+p}, 1, \quad (38b)$$

$$\Omega_\varphi = \frac{3}{\lambda_+^2}: \quad S \quad \text{with} \quad w_\varphi = 0. \quad (38c)$$

As follows from (11), the deceleration parameter is given by $q = (1 + 3w_\varphi\Omega_\varphi)/2$ and can be read off from the above values.

Finally, we notice that for the class of potentials under consideration the behaviour at late times of future accelerating models ($q < 0$) is of three possible types:

¹²Heuristically the situation is quite similar to when λ is bounded and $\lim_{\varphi \rightarrow -\infty} \lambda = \lambda_- \geq \sqrt{6}$, $\lim_{\varphi \rightarrow +\infty} \lambda = \lambda_+ \leq -\sqrt{6}$, as discussed in AUW [13]; in both cases the ‘scalar field particle’ is increasing its energy toward the past since there is friction toward the future, and in both cases the scalar field particle bounces infinitely many times between two steep potential walls toward the past, where the present potential wall at $\varphi = 0$ is even steeper than the potential wall in AUW [13] corresponding to $\lambda_- \geq \sqrt{6}$. It is therefore not surprising that in appropriate variables one can describe this phenomenon as a heteroclinic limit cycle, *i.e.* a cyclic chain of heteroclinic orbits.

- i) Monotonically decreasing potentials: if $0 < \lambda_+ < \sqrt{2}$ then the fixed point P is the sink, with $w_\varphi = \frac{\lambda_+^2}{3} - 1$ and $q = \frac{\lambda_+^2}{2} - 1$.
- ii) Monotonically decreasing potentials: if $\lambda_+ = 0$ then the fixed point dS is the sink, with $w_\varphi = -1$ and $q = -1$.
- iii) Potentials with a positive minimum: the fixed point dS⁰ is the sink, with $w_\varphi = -1$ and $q = -1$.

We conjecture, supported by heuristical arguments and numerical experiments, that in each case the sink is the *future global attractor*, denoted by \mathcal{A} , which thereby attracts all interior orbits, including those relevant for quintessence.

4 Quintessence

In this section we use the new dynamical system to describe and compare thawing, scaling freezing and tracking quintessence.

4.1 Observationally viable quintessence models

The first step is to identify which orbits in the ski-slope state space $(\bar{\varphi}, u, v)$ that describe observationally viable quintessence models. We begin with two necessary conditions:

- The model must be *accelerating at present and late times*, i.e. $q < 0$, where q is given by (11).
- The model must have an *early long matter-dominated epoch* ($\Omega_\varphi \lesssim 0.03$ for $\Delta N \sim 10$, see AUW [17]) and satisfy $\Omega_\varphi \approx 0.68$ at the present time $N = 0$.

First we identify the orbits in the state space that begin at matter-dominated fixed points and then end at the future attractor \mathcal{A} . Then we regard these unstable manifolds as reference orbits in the sense that *initial data sufficiently close to a fixed point of a viable reference orbit also provide viable quintessence models*. Referring to (38) we see that the relevant fixed points are FL₀ ^{φ_*} with $0 < \bar{\varphi}_* < 1$, T, and also S if the potential has a positive minimum and $\lambda_+ \ll -1$. For a given potential belonging to the present class of potentials with unbounded $\lambda(\varphi)$ there are thereby three possibilities for reference orbits for generating viable quintessence models, which we denote symbolically as follows:

- i) a one parameter family of reference orbits FL₀ ^{φ_*} $\rightarrow \mathcal{A}$ with $0 < \bar{\varphi}_* < 1$,
- ii) a single reference orbit S $\rightarrow \mathcal{A} = \text{dS}^0$ when $\lambda_+ \ll -1$,
- iii) a single reference orbit T $\rightarrow \mathcal{A}$,

where the future attractor \mathcal{A} for monotonically decreasing potentials is given by dS, P when $\lambda_+ = 0$, $0 < \lambda_+ < \sqrt{2}$, respectively, while $\mathcal{A} = \text{dS}^0$ when the potential has a positive minimum. The reference orbits in all three cases are the unstable manifolds of

the fixed points from which they originate. As we will see, the three sets of fixed points $\text{FL}_0^{\varphi^*}$, S and T have stable manifolds that push nearby orbits (corresponding to open sets of initial data near the fixed points) to the unstable manifold orbits which they subsequently shadow until they all end at the future attractor \mathcal{A} . Next we discuss the three cases, which correspond to thawing, scaling freezing and tracking quintessence, respectively, in more detail.

Thawing quintessence

In case i) each fixed point of $\text{FL}_0^{\varphi^*}$ has one eigenvalue that is zero (corresponding to the line of fixed points), one that is positive, which yields one reference orbit $\text{FL}_0^{\varphi^*} \rightarrow \mathcal{A}$ for each fixed point of $\text{FL}_0^{\varphi^*}$ (the unstable manifold of $\text{FL}_0^{\varphi^*}$), and one negative eigenvalue corresponding to the stable manifold $v = 0$ of $\text{FL}_0^{\varphi^*}$ on which $\bar{\varphi}$ is constant/‘frozen’, shown in Figure 1. The condition of a long matter-dominated epoch is *very* restrictive and leads to initial data with $0 < v \ll 1$, which result in open sets of orbits that are attracted/pushed toward to the unstable manifold reference orbits of $\text{FL}_0^{\varphi^*}$, which they subsequently very closely shadow, until they all end at the future attractor \mathcal{A} . Note further that the equation of state for the reference orbits starts at $w_\varphi \approx -1$ ($w_\varphi = -1$ at $\text{FL}_0^{\varphi^*}$) and then increases, which identify the reference orbits (and the orbits that shadow them) as *thawing quintessence* solutions.¹³ We discussed and elaborated on this type of quintessence in a dynamical systems setting for potentials with bounded λ in AUW [13] and notice that the situation for thawing quintessence is quite similar in the present case with unbounded λ .

Scaling freezing quintessence

Case ii) occurs for a potential with a positive minimum. A matter-dominated scaling epoch for such potentials, where ρ_φ approximately scales in time as ρ_m , only holds for an open set of interior initial data sufficiently close to the fixed point S. Moreover, since matter-dominance requires $\Omega_\varphi \lesssim 0.03 \Rightarrow v \lesssim 0.1$ and since $v|_S = 1/|\lambda_+|$ it follows that matter-dominated scaling orbits require $\lambda_+ \lesssim -10$. The fixed point S has two negative eigenvalues with the boundary $\bar{\varphi} = 1$ as the stable manifold on which S attracts all orbits, and one positive eigenvalue, which makes S a saddle point in the full state space, where the reference orbit $S \rightarrow dS^0$ is the unstable manifold associated with the positive eigenvalue. The open set of interior matter-dominated scaling initial data sufficiently close to S first approach S and then the reference orbit, which they then shadow, and then they all finally end at dS^0 . Due to that these orbits, and the reference orbit, exhibit the scaling property during the matter-dominated epoch near S where $w_\varphi \approx w_m = 0$, and since $w_\varphi = -1$ at dS^0 , these orbits correspond to *scaling freezing quintessence* solutions, see *e.g.* Tsujikawa (2013) [4].

Tracking quintessence

In this paper we focus on case iii). The fixed point T has two eigenvalues with negative real parts with the matter dominant boundary $\bar{\varphi} = 0$ as its stable manifold on which

¹³See, for example Chiba *et al.* (2013) [18], the introduction.

T attracts all orbits and one positive eigenvalue, making T a saddle point in the full state space where the positive eigenvalue yields the unstable manifold reference orbit $T \rightarrow \mathcal{A}$.

Since, according to (30), $\Delta = \bar{\varphi}\lambda(\bar{\varphi})v/u = G(\bar{\varphi})v/u$ where $G(0) = pb$, $u_T = pbv_T$, it follows that $\Delta = 1$ at the fixed point T, *i.e.* the first tracker condition is exactly fulfilled at T. Since we can write $\lambda = (p/\varphi)f(\varphi)$, where f is regular and satisfies $f(0) = 1$ due to the boundedness condition (17a) and since $\Gamma = 1 - \lambda_{,\varphi}/\lambda^2$ it follows that $\Gamma - 1 = 1/p > 1$ when $\varphi \rightarrow 0$ and hence at T, while $w_\varphi|_T = u_T^2 - 1 = -2/(2+p) < 0$ and thus the second tracker condition is also fulfilled at T. We therefore refer to T as the *tracker fixed point* and the unstable manifold reference orbit of T as the *tracker orbit*. When $w_\varphi(N)$ is nearly constant, which is true near T,¹⁴ the graph of $w_\varphi(N)$ has a horizontal plateau $w_\varphi \approx -2/(2+p)$, as illustrated in the graphs of $w_\varphi(N)$ in section 5.

If $\bar{\varphi}$ is sufficiently close to the matter dominant boundary $\bar{\varphi} = 0$ this results in an open set of initial conditions that yields orbits with a long matter-dominated epoch where they a) shadow the orbits on $\bar{\varphi} = 0$, see Figure 1(b), b) then approach and spiral around T, where they still are matter-dominated but where being close to T also implies that the orbits approximately obey the tracker conditions,¹⁵ c) and where they subsequently track/shadow the tracker orbit until they all end at the future attractor \mathcal{A} . Steinhardt *et al.* (1999) [7] characterizes the open set of orbits that track/shadow the tracker orbit as undershooting and overshooting orbits. In terms of our state space description this characterization is based on solutions with initial data close to $\bar{\varphi} = 0$ with $u \lesssim 0$, $0 \lesssim v < v_T$ (undershooting solutions), and $u \gtrsim 0$, $v \gg v_T$ (overshooting solutions). We will give specific examples in section 5.

In this way, to quote Steinhardt *et al.* (1999) [7] (see the introduction), who dealt with monotonically decreasing potentials for which $\lambda_+ = 0$, primarily the inverse power-law potential: "...a very wide range of initial conditions rapidly converge to a common, cosmic evolutionary track." However, it is worth noticing that for monotonically decreasing potentials with $\mathcal{A} = dS$ the fixed point dS has an eigenvalue that is zero with a stable interior state space center manifold direction, and two eigenvalues with negative real parts with the boundary $\bar{\varphi} = 1$ as their associated stable manifold. As a consequence *all* orbits are strongly attracted to the center manifold of dS, which means that they *all* 'track' each other, including tracking/shadowing the tracker orbit.

Finally, we comment on the dynamical systems approach by Bahamonde *et al.* (2018) used in [5] to study tracking quintessence for the inverse power-law potential. To do so they introduced variables that result in a non-regular system that breaks down when $\varphi \rightarrow 0$ (when their variable z is one, see their eqs. 4.37-4.38). They then regularize their equations by changing the time variable to obtain the system 4.40-4.42. However, this hides that the new time variable asymptotically breaks down when $\varphi \rightarrow 0$ and that their variables deform and crush our regular dynamical system at $\bar{\varphi} = 0$. This results in half circles at $z = 1$ and a fixed point at the intersection of two lines of fixed points at $x = 0$ on the line of fixed points B_x , see Figure 9 in [5]. The

¹⁴As we will see in section 5, there is a special class of models for which $w_\varphi = \text{constant}$ holds for the entire tracker orbit, but this is a very special class of models.

¹⁵Note, however, that the scalar field effectively is a test field not affecting the space-time geometry during matter-dominance.

eigenvalues at this fixed point are all zero, see Table 7 in [5]. The authors then perform a numerical investigation that suggests that the tracker orbit originates from the fixed point $x = 0$ on B_x .

In contrast to our regularized dynamical system with a time variable that does not break down when $\varphi \rightarrow 0$, the variables and dynamical system 4.40-4.42 in [5] cannot be used to: 1) explain the tracking attractor feature, which our variables show is due to that $\bar{\varphi} = 0$ is the stable manifold of T, 2) nor can the dynamical system 4.40-4.42 be used to obtain analytic approximations for the tracker orbit since all eigenvalues are zero at $x = 0$ on B_x , while we will use the unstable manifold corresponding to the positive eigenvalue at T to obtain simple and accurate approximations for tracker orbits for a wide range of potentials in a future follow up paper.

4.2 Thawing, scaling freezing and tracking quintessence

We conclude this section with some further comments on thawing, scaling freezing and tracking quintessence for a potential with unbounded λ . We first note that there is a close mathematical relationship between the present models with unbounded $\lambda(\varphi)$ and tracking quintessence and models with bounded $\lambda(\varphi)$ that have a very large λ_- and thereby admit scaling quintessence associated with $\varphi \rightarrow -\infty$. The two cases have a fixed point T and S, respectively, with stable manifolds on a boundary associated with their respective scalar field limits, and both have a single reference orbit as their unstable manifold that attracts an open set of orbits that come close to the fixed point; cf. AUW [13] with the present paper, especially the illustrative figures in AUW and in the next section. However, recall that $\Omega_\varphi = 3/\lambda_+^2$, $1 \ll |\lambda_+|$ and hence $0 < \Omega_\varphi \ll 1$ at S for scaling freezing quintessence while $\Omega_\varphi = 0$ for tracking (and thawing) quintessence at T (and $\text{FL}^{\varphi*}$).

We finally comment on the distinction between tracking, scaling freezing and thawing quintessence, which is not as clear cut as it first appears. We first note that scalar field potentials *always* give rise to an open set of thawing quintessence solutions (where some of the thawing solutions are observationally compatible with the Λ CDM model if a scalar field potential has a sufficiently slowly changing part) shadowing the thawing quintessence reference orbits. If the present class of potentials exhibits a positive minimum and $\lambda_+ \ll -1$ then apart from the open sets of orbits that exhibit thawing and tracking quintessence there also exists an open set of scaling freezing quintessence orbits. The coexistence of thawing quintessence with tracking and also scaling freezing quintessence (if the potential has a minimum and $\lambda_+ \ll -1$) causes complications as regards distinguishing thawing quintessence from tracking and scaling freezing quintessence. This complication is caused by the orbits $\text{FL}_0 \rightarrow \text{T}$ and $\text{FL}_0 \rightarrow \text{S}$ in the boundary sets $\bar{\varphi} = 0$ and $\bar{\varphi} = 1$, respectively. It follows that the unstable manifold of any fixed point $\text{FL}_0^{\varphi*}$ with $0 < \bar{\varphi}_* \ll 1$ ($0 \ll \bar{\varphi}_* < 1$) will shadow the orbit $\text{FL}_0 \rightarrow \text{T}$ ($\text{FL}_0 \rightarrow \text{S}$) and hence pass close to T (S), giving rise to solutions that are both thawing and tracking (scaling freezing) quintessence models. To avoid this ambiguity we impose the restriction $0 \ll \bar{\varphi}_* < 1$ (and $0 \ll \bar{\varphi}_* \ll 1$ for potentials with a minimum and $\lambda_+ \ll -1$) when describing thawing quintessence models.

5 Numerical simulations for tracking quintessence

Instead of using the inverse power-law potential as an illustrative example, we use the following more versatile class of hyperbolic potentials:

$$V = V_0 \left[\frac{\nu(\cosh \nu\varphi)^{1-\alpha}}{\sinh(\nu\varphi)} \right]^p \quad \Longrightarrow \quad \lambda = \frac{p\nu}{\tanh \nu\varphi} [1 + (\alpha - 1)(\tanh \nu\varphi)^2], \quad (39)$$

where $\varphi \in (0, \infty)$, $p > 0$, $\nu > 0$, while α is arbitrary, and

$$\lambda_+ = p\nu\alpha. \quad (40)$$

For these models a suitable choice of $\bar{\varphi}$ is

$$\bar{\varphi} = \tanh(\nu\varphi) \quad \Longrightarrow \quad F(\bar{\varphi}) = \nu(1 - \bar{\varphi}^2), \quad (41)$$

satisfying (19) with $b = \nu$, which leads to

$$G(\bar{\varphi}) = p\nu [1 + (\alpha - 1)\bar{\varphi}^2], \quad \Gamma - 1 = \frac{(1 - \bar{\varphi}^2)(1 - (\alpha - 1)\bar{\varphi}^2)}{p[1 + (\alpha - 1)\bar{\varphi}^2]^2}, \quad (42)$$

where $\Gamma > 1$ globally if $\alpha < 2$. The special cases $\alpha = 1$ and $\alpha = 0$ with $V \propto \sinh^{-p}(\nu\varphi)$ and $V \propto \tanh^{-p}(\nu\varphi)$, respectively, are well known.¹⁶

We note that if we use the illustrative positive potential (39) a minimum of such a potential implies that $\alpha < 0$ and where the fixed point dS^0 is located at $\bar{\varphi}_0 = 1/\sqrt{1 - \alpha}$. In order for dS^0 not only to be a sink but a spiral sink it follows that $p\nu^2\alpha < -3/8$, which follows from the spiral condition $\lambda_{,\varphi}|_{\bar{\varphi}=\bar{\varphi}_0} < -3/4$ in footnote 11 where $\lambda_{,\varphi}|_{\bar{\varphi}=\bar{\varphi}_0} = 2p\nu^2\alpha$ for the present models. We will use these models to illustrate that there are three types of tracker orbits for potentials that are monotonically decreasing: those for which w_φ is overall decreasing, constant, and increasing, and then we will turn to the case of a potential with a positive minimum.

5.1 Monotonic potentials: Three types of tracker orbits

The central features for tracking quintessence are the tracker fixed point T and the tracker orbit $\text{T} \rightarrow \mathcal{A}$, where \mathcal{A} is one of the fixed points P , dS for monotonically decreasing potentials depending on whether $0 < \lambda_+ < \sqrt{2}$ or $\lambda_+ = 0$, respectively. We then note that

$$1 + w_\varphi|_{\text{T}} = u_{\text{T}}^2 = \frac{p}{2+p}, \quad 1 + w_\varphi|_{\text{P/dS}} = u_{\text{P/dS}}^2 = \frac{1}{3}\lambda_+^2 = \frac{1}{3}(p\nu\alpha)^2, \quad (43)$$

where the last equality follows from (40). Hence the overall decrease/increase of w_φ for the tracker orbit $\text{T} \rightarrow \mathcal{A}$ is determined by the values of u_{T} and u_{P} (or, possibly, u_{dS}

¹⁶See Urena-Lopez and Matos (2000) [19] and Bag *et al.* (2018) [20].

when w_φ is overall decreasing), which leads to:

$$\sqrt{3}u_T = \sqrt{\frac{3p}{2+p}} > \sqrt{3}u_{P/dS} = \lambda_+, \quad \text{overall decrease in } w_\varphi, \quad (44a)$$

$$\sqrt{3}u_T = \sqrt{\frac{3p}{2+p}} = \sqrt{3}u_P = \lambda_+, \quad \text{overall constant } w_\varphi, \quad (44b)$$

$$\sqrt{3}u_T = \sqrt{\frac{3p}{2+p}} < \sqrt{3}u_P = \lambda_+, \quad \text{overall increase in } w_\varphi, \quad (44c)$$

where we recall that $\lambda_+ = p\nu\alpha$ for the potentials (39).

It does not follow in general that w_φ is constant during the evolution for the borderline case (44b), although there is no overall change in w_φ during the evolution from T to P. However, suitable restrictions on the parameters α, p, ν for the potentials (39) give rise to a subclass of potentials for which $w_\varphi = u^2 - 1$ is constant for a particular solution. In the early years of quintessence, Sahni and Starobinsky (2000) [21], equation (121), and Urena-Lopez and Matos (2000) [19], investigated models with the potential (39) with $\alpha = 1$, *i.e.* $V \propto \sinh^{-p}(\nu\varphi)$, and pointed out that these models admitted a special solution for which w_φ is constant. This model corresponds to the tracker orbit when $w_\varphi|_T = w_\varphi|_P$ and hence $\sqrt{3}u_T = \sqrt{3}u_P = \lambda_+ = p\nu$, where the last equality follows from setting $\alpha = 1$ in (40), which results in $\sqrt{3p/(2+p)} = p\nu$, and hence

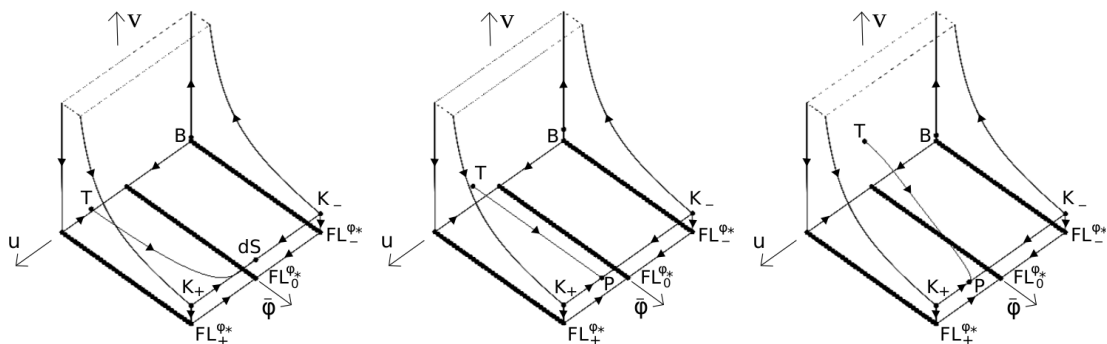
$$\nu = \sqrt{\frac{3}{p(2+p)}}. \quad (45)$$

Positive potentials $V \propto \sinh^{-p}(\nu\varphi)$ with any value of $p > 0$ and the above value of ν result in that the tracker orbit $T \rightarrow P$ is a straight line in the state space $(\bar{\varphi}, u, v)$, parallel to the $\bar{\varphi}$ axis given by $u = u_T = \sqrt{p/(2+p)}$, $v = v_T = u_T/p\nu = 1/\sqrt{3}$, and thereby with a constant w_φ given by $1 + w_\varphi = u_T^2 = p/(2+p)$. Furthermore, since $\Omega_\varphi = 3v^2\bar{\varphi}^2$ it follows that $\Omega_\varphi = \bar{\varphi}^2$.

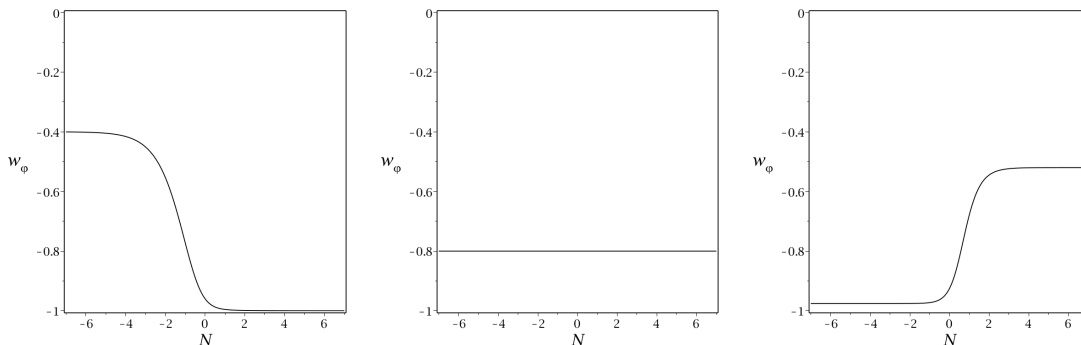
Along *any* of the above three types of tracker orbits, the graph of w_φ begins during matter-dominance ($\Omega_\varphi \approx 0$) close to T with a horizontal plateau $w_\varphi \approx -2/(2+p)$, *i.e.* $-1 < w_\varphi < 0$. During the evolution Ω_φ thereby starts close to zero near T and then increases to 1 at \mathcal{A} . The present epoch at $N = 0$ is characterized by that $\Omega_\varphi(N)$ reaches the observed value $\Omega_\varphi(0) = \Omega_{\varphi,0} \approx 0.68$. The value of w_φ at late times depends on \mathcal{A} but its value at the present time depends on $\lambda(\bar{\varphi})$ at $\bar{\varphi}(N = 0)$. For monotonically decreasing potentials with $\lambda_+ = 0$ the tracker orbit approaches dS and hence $w_\varphi \rightarrow -1$ asymptotically, but is greater than -1 when $N = 0$. These features are illustrated in Figure 3.

5.2 The tracker orbit for a potential with a minimum

In this case $T \rightarrow dS^0$ where the sink dS^0 resides on the matter dominant boundary $v\bar{\varphi} = 1/\sqrt{3}$ with $\bar{\varphi} = \bar{\varphi}_0$ determined by $\lambda(\bar{\varphi}_0) = 0$. If $\lambda_{,\varphi}|_{\bar{\varphi}=\bar{\varphi}_0} < -3/4$, then, according to footnote 11, dS^0 is a spiral focus sink in the boundary set $v\bar{\varphi} = 1/\sqrt{3}$ (see Figures 2 and 4). The fixed point dS^0 has another feature which helps to describe how the orbits are attracted to dS^0 , including the tracker orbit. There is an orbit $FL_0^{\varphi*} \rightarrow dS^0$ that is a



(a) Tracker orbit for the potential (39) with $\alpha = 0$, and $\nu = p = 3$. (b) Tracker orbit for the potential (39) with $\alpha = 1$, $\nu = \sqrt{\frac{12}{5}}$ and $p = 0.5$. (c) Tracker orbit for the potential (39) with $\alpha = 12$, $\nu = 2$ and $p = 0.05$.



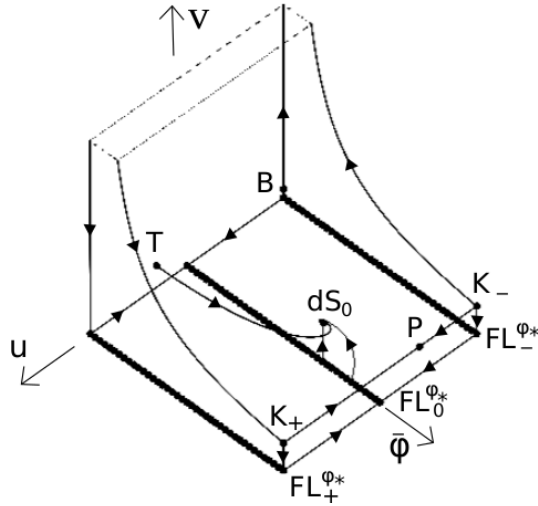
(d) Decreasing $w_\varphi(N)$ for the tracker orbit with a potential (39) with $\alpha = 0$, and $\nu = p = 3$. (e) Constant $w_\varphi(N)$ for the tracker orbit with a potential (39) with $\alpha = 1$, $\nu = \sqrt{\frac{12}{5}}$ and $p = 0.5$. (f) Increasing $w_\varphi(N)$ for the tracker orbit with a potential (39) with $\alpha = 12$, $\nu = 2$ and $p = 0.05$.

Figure 3: Tracker orbits in the ski-slope state-space and the respective graph of $w_\varphi(N)$ for the potential (39), illustrating that w_φ can decrease, be a constant, and increase for the tracker orbit.

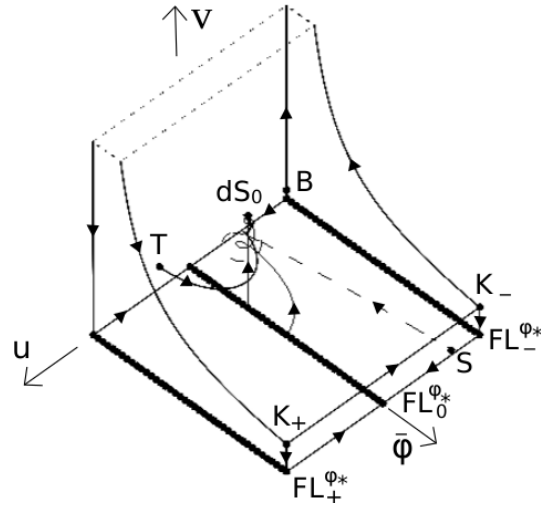
straight line characterized by $\bar{\varphi} = \bar{\varphi}_* = \bar{\varphi}_0$, $u = 0$, $0 < v < 1/\sqrt{3}$. This orbit describes the Λ CDM solution, which corresponds to that the scalar field resides in the positive minimum of the potential, where $\lambda(\bar{\varphi}_0) = 0 = G(\bar{\varphi}_0)$, giving rise to $\Lambda = V(\bar{\varphi}_0) > 0$. All interior orbits are asymptotic to the spiral (assuming that $\lambda_{,\varphi}|_{\bar{\varphi}=\bar{\varphi}_0} < -3/4$) sink dS^0 and hence as they come close to dS^0 they spiral around the Λ CDM orbit. In particular, the tracker orbit $T \rightarrow dS^0$ originates from T with $\Delta \approx 1$, $w_\varphi \approx \text{constant}$ and then it bends and eventually forms a spiral around the Λ CDM orbit as it approaches dS^0 . These features are illustrated in Figure 4.

5.3 Tracking quintessence for an open set of initial data

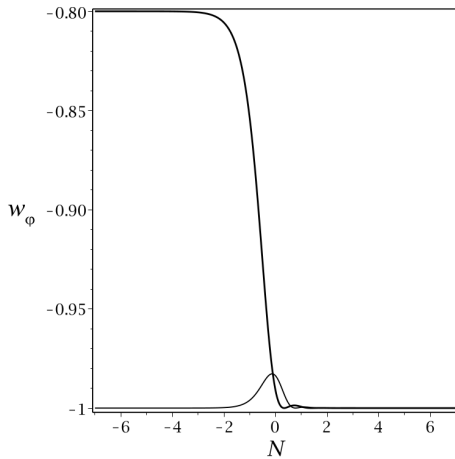
Recall that Steinhardt *et al.* (1999) [7] characterized the open set of orbits tracking/shadowing the tracker orbit as undershooting and overshooting orbits, which corresponds to $u \lesssim 0$, $0 \lesssim v < v_T$ (undershooting solutions) and $u \gtrsim 0$, $v \gg v_T$ (overshooting solutions), where the condition of a long matter-dominated epoch requires



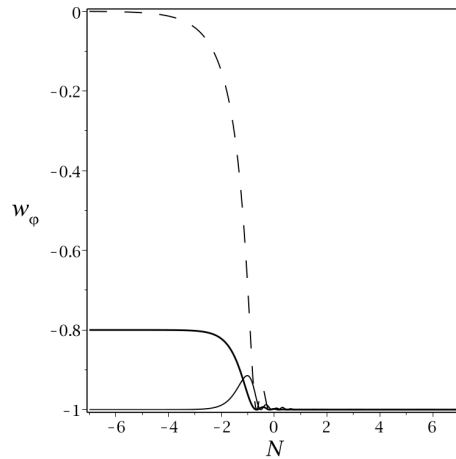
(a) Tracker, Λ CDM, and a thawing quintessence orbit for the potential (39) with $\nu = 2$, $p = 1/2$, and $\alpha = -1$.



(b) Tracker, Λ CDM, scaling freezing, and a thawing quintessence orbit for the potential (39) with $\alpha = -10$, $\nu = 2$ and $p = 1/2$.



(c) Graphs of w_φ for the tracker and thawing quintessence orbits for the potential (39) with $\nu = 2$, $p = 1/2$, and $\alpha = -1$.



(d) Graphs of w_φ for the tracker, thawing and scaling freezing quintessence orbits for the potential (39) with $\nu = 2$, $p = 1/2$, and $\alpha = -10$.

Figure 4: The tracker orbit in the ski-slope state-space and their graphs $w_\varphi(N)$ for the potential (39) with a minimum, together with the Λ CDM orbit, a thawing quintessence reference orbit originating from $FL_0^{\varphi*}$, and also a scaling freezing quintessence reference orbit when $\lambda_+ \ll -1$ in figure (b), with associated graphs of w_φ in (c) and (d), where w_φ for the thawing orbit begins with $w_\varphi \approx -1$, while the tracker orbit begins with $w_\varphi \approx -2/(2+p)$, which for $p = 1/2$ yields $w_\varphi \approx -0.8$, and where the dashed scaling freezing orbit begins with $w_\varphi \approx 0$.

these conditions for initial data to be supplemented by a very small value of $\bar{\varphi}$ near the $\bar{\varphi} = 0$ matter dominant boundary.¹⁷ Solutions corresponding to such initial data

¹⁷Note that $u < 0$ results in $\bar{\varphi}' < 0$, which means that the boundary $\bar{\varphi} = 0$ is stable (attracts nearby orbits), while $u > 0$ yields $\bar{\varphi}' > 0$ and that $\bar{\varphi} = 0$ is unstable. The u -dependent stability properties

shadow orbits on the $\bar{\varphi} = 0$ boundary, where we can use Figure 1(b) to obtain a feeling for how the solutions behave before they begin to spiral around T in its vicinity during the matter-dominated epoch. Since $w_\varphi = u^2 - 1$ this also gives a feeling for how graphs of w_φ behave, however, recall that the scalar field is essentially a test field during the matter-dominated epoch and hence that this behaviour of w_φ is not an observable property and thereby physically unimportant. These features are illustrated in Figure 5. The graph $w_\varphi(N)$ in Figure 5(c) of the overshooting (dashed) orbit in Figures 5(a) and 5(b) covers the stage when it is very close to the boundary orbit at $\bar{\varphi} = 0$, $u = \sqrt{2}$ where $w_\varphi = 1$ (earlier it shadowed an orbit on the $\bar{\varphi} = 0$ boundary that passed $u = 0$ at a very large value of v not shown), subsequently, due to that $\bar{\varphi}' > 0$, it shadows a nearby orbit on the $u = \sqrt{2}$ boundary, see Figure 5(b), which is followed by shadowing an orbit $\text{FL}_+^{\varphi*} \rightarrow \text{FL}_0^{\varphi*}$ with $\bar{\varphi} = \text{constant} \ll 1$, and then an unstable $\text{FL}_0^{\varphi*}$ reference orbit near the orbit $\text{FL}_0^{\varphi*} \rightarrow \text{T}$ on $\bar{\varphi} = 0$,¹⁸ and finally it shadows the tracker orbit $\text{T} \rightarrow \text{dS}$;¹⁹ the graph $w_\varphi(N)$ in Figure 5(c) of the undershooting (dotted) orbit in Figures 5(a) and 5(b) covers the stage when this undershooting orbit shadows an orbit on the $\bar{\varphi} = 0$ boundary when it passes $u = 0$ where $w_\varphi = -1$ and afterwards where it, due to that $\bar{\varphi}' < 0$ when $u < 0$, comes extremely close to T and where it subsequently shadows the tracker orbit $\text{T} \rightarrow \text{dS}$ (both the overshooting and undershooting orbits basically overlap with the tracker orbit after the matter-dominated tracker stage, where the tracker solution therefore describes the quintessence epoch of the overshooting and undershooting solutions extremely well).

6 Concluding remarks

We have given, for the first time, a description of tracking quintessence in a *regular* state space framework using the e -fold time N , showing that it is generated by any potential for which λ is unbounded with $\varphi\lambda \rightarrow p > 0$ as $\varphi \rightarrow 0$. A central role is played by a unique tracker orbit that originates from the tracker fixed point T which then governs the transition from matter-domination to quintessence-domination and an accelerating universe. Our state space provides some clarification for the claim of Steinhardt *et al.* (1999) [7] that with tracking quintessence, "a very wide range of initial conditions rapidly converge to a common, cosmic evolutionary track of $\rho_\varphi(N)$ and $w_\varphi(N)$ ".

We have shown that potentials with unbounded λ also lead to thawing and scaling freezing quintessence (the latter for potentials with a positive minimum and $\lambda_+ \ll -1$) and have used the state space to make a distinction between the three types, based on which fixed points the reference orbits originate from (cf. with the more complicated

of $\bar{\varphi} = 0$ imply that undershooting solutions begin tracking sooner than overshooting solutions, see Figure 5 and Figure 5 in Steinhardt *et al.* (1999) [7].

¹⁸This sequence of shadowing orbits is approximately described by shadowing a certain orbit on the $\bar{\varphi} = 0$ boundary, where the approximation is improved by choosing a smaller $\bar{\varphi}$ datum.

¹⁹Note, as follows from Figure 5(c), the (dashed) overshooting solution only obeys the tracker conditions for a short while between approximately $N = -5$ to $N = -3$. To increase this time period requires an even smaller initial value of $\bar{\varphi}$ than presently, so that the orbit comes closer to T. Note also that this overshooting orbit illustrates the ambiguity between thawing and tracker quintessence discussed in the previous section, since it shadows an unstable $\text{FL}_0^{\varphi*}$ orbit during a thawing epoch.

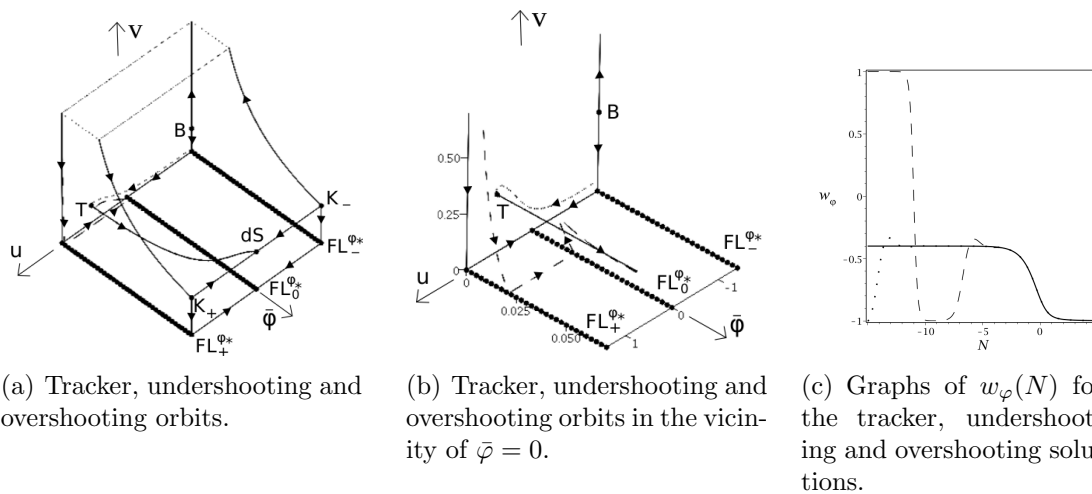


Figure 5: The tracker orbit (full line), overshooting (dashed line) and undershooting (dotted line) orbits in the ski-slope state-space and their graphs $w_\varphi(N)$ for the monotonically decreasing positive potential (39) with $\nu = 1$, $p = 3$ and $\alpha = 0$.

classification used in AUW[13]). One might ask: *Which of the open sets of different types of quintessence initial data is preferred? Why should tracking quintessence have a special status?*

Finally, we note that the present dynamical systems formulation can be slightly modified to obtain simple and accurate approximations with the Λ CDM model as a continuous parameter/initial data limit for tracking and thawing quintessence,²⁰ which will be the topic of a forthcoming paper.

Acknowledgments

A. A. is supported by FCT/Portugal through CAMGSD, IST-ID, projects UIDB/04459/2020 and UIDP/04459/2020, and by the H2020-MSCA-2022-SE project EinsteinWaves, GA No. 101131233. A.A. would also like to thank the CMA-UBI in Covilhã for kind hospitality. C. U. would like to thank the CAMGSD, Instituto Superior Técnico in Lisbon for kind hospitality.

References

- [1] A. G. Riess et al. Observational evidence from supernovae for an accelerating universe and a cosmological constant. *Astron. J.*, **116**:1009, 1998.
- [2] S. Perlmutter et al. Measurements of omega and lambda from 42 high redshift supernovae. *Astron. J.*, **517**:565, 1999.

²⁰This is not possible for scaling freezing quintessence since $w_\varphi = w_m = 0$ at S and not $w_\Lambda = -1$, although it is possible to obtain approximate solutions for scaling freezing quintessence in the same manner as we will accomplish for thawing and tracker quintessence.

- [3] R. R. Caldwell, Rahul Dave, and Paul J. Steinhardt. Cosmological imprint of an energy component with general equation of state. *Phys. Rev. Lett.*, **80**:1582–1585, 1998.
- [4] S. Tsujikawa. Quintessence: a review. *Class. Quantum Grav.*, **30**:214003, 2013.
- [5] S. Bahamonde, C. G. Böhm, S. Carloni, E. J. Copeland, Wei Fang, and N. Tamanini. Dynamical systems applied to cosmology: Dark energy and modified gravity. *Physics Reports*, **775-777**:1–122, 2018.
- [6] I. Zlatev, L. Wang, and P. J. Steinhardt. Quintessence, cosmic coincidence and the cosmological constant. *Phys. Rev. Lett.*, **82**:896, 1999.
- [7] P. J. Steinhardt, L. Wang, and I. Zlatev. Cosmological tracking solutions. *Phys. Rev. D*, **59**:123504, 1999.
- [8] P. J. E. Peebles and B. Ratra. Cosmology with a time variable cosmological constant. *Astro. Phys. J.*, **325**:L17, 1988.
- [9] B. Ratra and P. J. E. Peebles. Cosmological consequences of a rolling homogeneous scalar field. *Phys. Rev. D*, **37**:3406, 1988.
- [10] B. Ratra and A. Quillen. Gravitational lensing effects in a time-variable cosmological ‘constant’ cosmology. *Monthly Notices of the Royal Astronomical Society*, 259(4):738–742, 12 1992.
- [11] S. Podariu and B. Ratra. Supernova ia constraints on a time-variable cosmological “constant”. *The Astrophysical Journal*, 532(1):109, mar 2000.
- [12] P. J. E. Peebles and Bharat Ratra. The cosmological constant and dark energy. *Rev. Mod. Phys.*, **75**:559–606, 2003.
- [13] A. Alho, C. Uggla, and J. Wainwright. Quintessence from a state space perspective. *Physics of the Dark Universe*, **39**:101146, 2023.
- [14] A. Alho and C. Uggla. Quintessential α -attractor inflation: A dynamical systems analysis. *Journal of Cosmology and Astroparticle Physics*, **11**:083, 2023.
- [15] A. Alho and C. Uggla. Scalar field deformations of lambda-cdm cosmology. *Phys. Rev. D*, **92**(10):103502, 2015.
- [16] C. Rubano, P. Scudellaro, and E. Piedipalumbo. Exponential potentials for tracker fields. *Phys. Rev. D*, **69**:103510, 2004.
- [17] A. Alho, W. C. Lim, and C. Uggla. Cosmological global dynamical systems analysis. *Class. Quantum Grav.*, **39**:145010, 2022.
- [18] T. Chiba, A. De Felice, and S. Tsujikawa. Observational constraints on quintessence: Thawing, tracker and scaling models. *Phys. Rev. D*, **87**:083505, 2013.

- [19] L.A. Urena-Lopez and T. Matos. New cosmological tracker solution for quintessence. *Phys. Rev. D*, **62**:081302, 2000.
- [20] S. Bag, S.S. Mishra, and V. Sahni. New tracker models of dark energy. *Journal of Cosmology and Astroparticle Physics*, **08**:009, 2018.
- [21] V. Sahni and A.Starobinsky. The case for a positive cosmological lambda-term. *Int. J. Mod. Phys. D*, **9**:373, 2000.